Estimation of annual regional drought index considering the joint effects of climate and water budget for Krishna River basin, India

by

Shaik Rehana, Monish N.T., Sireesha Naidu.G

in

Environ Monit Assess

Report No: IIIT/TR/2020/-1

Centre for Spatial Informatics
International Institute of Information Technology
Hyderabad - 500 032, INDIA
May 2020

Environ Monit Assess (2020) 192:427
https://doi.org/10.1007/s10661-020-08379-y

Estimation of annual regional drought index considering the joint effects of climate and water budget for Krishna River basin, India

Rehana Shaik · Monish N.T. · Sireesha Naidu G.

Received: 9 September 2019 / Accepted: 21 May 2020

Abstract The Standardized Precipitation and Evapotranspiration Index (*SPEI*) became one of the popular drought indices due to the consideration of difference between precipitation (*P*) and potential evapotranspiration (*PET*), which represents the energy-based climatic water balance. Implementation of actual evapotranspiration (*AET*), which accounts for both water and energy-based climatic evaporative demand in drought characterization studies, is limited. This study proposes a meteorological drought index with the structure of the *SPEI* and actual evapotranspiration modeled with empirical formulations and remote sensing data integrated with surface energy models at annual scale. The proposed drought index imposes the effect of precipitation, *PET*, and *AET* using operational meteorological data sets of precipitation and temperatures. The present study aimed to test how a drought index based on *PET* and *P* can outperform with the inclusion of *AET* at a river basin scale at 12-month scale. The proposed hypothesis was tested considering Krishna River basin, India, as a case study for which most of the basin is in arid climate. The performance of drought indices was compared using historical droughts in terms of severity, areal extent, frequency, and duration based on empirical *AET* models along with satellite-based land surface *ET* data-based drought indices. The proposed *AET*-based drought indices have effectively captured the historical drought years over the Krishna River basin. The empirical *AET* formulation-based drought index was identified as a more reliable measure in the estimation of drought characteristics by comparing with satellite-based land surface *AET*-based drought index. The *AET*-based drought indices were able to drive the areas into moderate, which or otherwise categorized under severe drought regions with *PET*-based drought indices. Inclusion of *AET* in the drought characterization along with precipitation and *PET* can drive the highly intensified drought events determined by *SPEI* into moderate and less frequent droughts with short durations over a large river basin with arid climate.

Keywords Budyko equation · Turc model · Remote sensing · Thornthwaite model · *SPEI* · SPAEI

Introduction

Among the extreme events, droughts are the most widespread and slowly developing atmospheric hazards which remain for a long duration affecting natural resources, environment, and people. Several drought indices have been developed, which evaluate the deviation of climate variables in a given year from the normal conditions (Dai, 2011; Liu et al., 2017). The most widely and tested worldwide drought index is Palmer Drought Severity Index (PDSI) developed by Palmer (1965) that considers precipitation, evapotranspiration, and soil water holding capacity. The applicability of PDSI is limited due to the computational complexity,

R. Shaik (✉) · M. N.T. · S. G.
Lab for Spatial Informatics, International Institute of Information Technology, Hyderabad 500032, India
e-mail: rehana.s@iiit.ac.in

Published online: 13 June 2020

requirement of significant meteorological data, and applicability on different time scales. One of the widely accepted drought indices by the World Meteorological Organization (WMO) is Standardized Precipitation Index (SPI) developed by McKee et al. (1993). SPI measures the drought index at different time scales and enable to detect different drought types and it is widely accepted in the research community for drought monitoring and early warning (e.g., Hayes et al., 1999). The Standardized Precipitation and Evapotranspiration Index (*SPEI*) has been proposed by Vicente-Serrano et al. (2010, 2011), which considers the potential evapotranspiration (*PET*) in addition to precipitation and it can be used at several time scales. Due to the consideration of *PET*, *SPEI* combines the sensitivity of PDSI and the probabilistic and multi-temporal nature of SPI. In recent years, the *SPEI* has been widely used to evaluate drought events worldwide (Allen et al. 2011, Aadhar and Mishra 2017) as well as for Indian subcontinent (Kumar et al. 2013; Mallya et al. 2016; Nath et al. 2017).

To this end, the use of *PET* in the drought estimation (e.g., *SPEI*) has been identified as a reliable measure to characterize droughts that would experience modest drying if only precipitation is considered (Cook et al. 2014). Although *PET*-based drought indices consider the climatic water demand, it is limited towards the inclusion of the effects of regional land surface changes and actual moisture availability in the drought estimation (Vicente-Serrano et al. 2010). However, *PET* is the maximum possible moisture loss limited only by the energy endowment or it is the energy-driven *ET* (Shelton, 2009), whereas the actual evapotranspiration (*AET*) represents the transfer of moisture from the surface to the atmosphere in response to both the energy demand and available moisture supply. Therefore, drought indices estimated based on *AET* will consider both climatic water demand and actual available moisture. The inclusion of *AET* in the drought index will also be useful to consider the joint effect of land surface changes or variability and water-energy balance (Liu et al., 2017). The efforts made in the literature to include *AET* in the drought indices are Drought Severity Index (DSI) (Mu et al., 2013) and U.S. Drought Monitor (USDM) (Svoboda et al., 2002). However, these indices use *AET* estimated using remote sensing datasets and vegetation information from normalized difference vegetation index (NDVI) and tries to account for land surface changes implicitly. Recently, Kim and Rhee (2016) developed Standardized Evapotranspiration Deficit Index (SEDI) using the *AET* estimated from Bouchet hypothesis and the structure of *SPEI* as a fully ET-based drought index without consideration of precipitation. Towards the inclusion of *AET* in meteorological drought assessment, few authors made effort to use hydrological model driven *AET* outputs in the drought index estimation (e.g., Narasimhan and Srinivasan, 2005; Homdee et al., 2016). Narasimhan and Srinivasan (2005) developed Evapotranspiration Deficit Index (ETDI), where a distributed hydrologic model, Soil Water Assessment Tool (SWAT), was used to model *AET*. Homdee et al. (2016) compared *SPEI* with *AET*-based drought indices, where *AET* was modeled based on SWAT. However, hydrological model driven *AET*-induced drought indices will provide a limitation over the applicability over large spatial scales given with the rigorous catchment characteristic requirements. Therefore, an *AET*-based drought index should be able to use operational meteorological data for the ease of drought assessment at various spatial and temporal scales and for the impact assessment under climate variability. For this purpose, empirical models which assume that *AET* is limited by the water availability in terms of precipitation under very dry conditions and energy availability in terms of *PET* under very wet conditions (Turc, 1954; Budyko, 1958; Fu, 1981; Milly, 1994; Zhang et al., 2004) could provide a promising solution. Among these *AET* models, widely used classical approach to estimate *AET* at river catchment scale relating precipitation and *PET* is Budyko (Budyko, 1958) model.

Thus, the present study aims to develop a meteorological drought index, named Standardized Precipitation Evapotranspiration Index ($SPAEI_{Budyko}$), based on *AET* estimated by the Budyko hypothesis and the structure of *SPEI*. The original Budyko equation was developed for long-time scales (e.g., Budyko, 1974; Zhou et al., 2015) and implication of the model lower than annual scale necessitates boundary conditions (Sposito, 2017) as the accumulated precipitation values tending to zero for dry months. Therefore, the present study adopted another empirical *AET* model with minimum data requirement developed by Turc (1954) and named as $SPAEI_{Turc}$. The comparison and validation of two *AET*-based drought indices enables to study the sensitivity of *AET* models on the drought characterization. Further, to study the strength of the proposed empirical *AET*-based drought indices in predicting the drought characteristics, the study used satellite-based land surface *ET* data with the *SPEI* formulation ($SPAEI_{RS\_ET}$). The drought characteristics over the river basin were compared in terms areal extent, severity, frequency, and duration with four drought indices: *PET*-based drought index as *SPEI*, *AET*-based drought index with Budyko formulation as ($SPAEI_{Budyko}$), *AET*-based drought index with Turc formulation as ($SPAEI_{Turc}$), *AET* based on remote sensing data as ($SPAEI_{RS\_ET}$). The proposed drought indices were used to characterize historical drought events over a large river basin, Krishna River basin (KRB), India, for which most of the basin is with arid climate.

Study area

The study was conducted on KRB, which is fifth largest river system in India. Krishna River basin occupies an area of 258,948 km^2 which is 8% of the total geographical area of the country. Nearly 44% lies in Karnataka, 26% of the basin falls in Maharashtra, about 15% in Telangana, and another 15% in Andhra Pradesh within the range 73° 17′–81° 9′ E and 13° 10′–19° 22′ N. The river originates in the Western Ghats and flows for about 1400 km before reaching to the Bay of Bengal. The major tributaries of the river are Ghataprabha, Malaprabha, Tunga-Bhadra, Bhima, Vedavathi, and Musi. There are two major cropping seasons: Kharif occurs from June to November and Rabi from December to March (George et al., 2011). Most of the Krishna River basin is covered by arid climate (Fig. 1) with annual average precipitation in the basin as 784 mm, of which approximately 90% occurs during the South-West Monsoon from June to October (http://india-wris.nrsc.gov.in/wrpinfo/?title=Krishna). Some parts of the Krishna River basin especially the Rayalaseema area of Andhra Pradesh, Bellary, Raichur, Dharwar, Chitradurga, Belgaum, and Bijapur districts of Karnataka and Pune, Sholapur, Osmanabad, and Ahmednagar districts of Maharashtra are drought-prone (source: http://india-wris.nrsc.gov.in/wrpinfo/index.php? title=Krishna) (Fig. 1).

Development of Standardized Precipitation-Actual Evapotranspiration Index

Conventionally, it is assumed that available water and energy are the primary factors affecting the rate of evapotranspiration (Budyko, 1958). In this context, the use of *PET* in the drought assessment studies may not be able to include the actual surface available moisture. Further, the *AET* includes the interception, actual soil evaporation, and actual plant transpiration (Homdee et al., 2016). If the difference between precipitation and *AET* is considered, it can account for the actual residual available water (*RAW*) or water budget during drought conditions.

Therefore, the water budget at a river basin scale can be expressed as

$$\Delta S = P + Q_{in} + GW_{in} - GW_{out} - Q_{out} - AET \tag{1}$$

where S is the storage volume, GW_{in} (GW_{out}) is the ground water inflow (outflow) volume, and Q_{in} (Q_{out}) is the surface runoff inflow (outflow) volume. For sufficiently long-time scales, the net change in storage volumes corresponding to ground water can be assumed to be zero. This will direct to a simplified water budget equation or actual residual water available (*RAW*) over a river basin, which can be expressed as follows:

$$RAW = P - AET \tag{2}$$

where *RAW*, *P*, and *AET* are in millimeters.

Estimation of actual evapotranspiration

Various empirical models have been developed for estimating *AET* which is based on the assumption that *AET* is limited by the water availability in terms of precipitation under very dry conditions and available energy under very wet conditions in terms of potential evapotranspiration (Budyko, 1958; Fu, 1981; Milly, 1994; Zhang et al., 2004).

AET estimation based on Budyko model

Budyko (1958) has developed a relationship between three hydro-climatic variables for a basin: precipitation (*P*), *PET*, and *AET*. The Budyko hypothesis states that the ratio of the *AET* over precipitation (*AET*/*P*) is fundamentally related to the ratio of the *PET* over precipitation (*PET*/*P*) (Budyko 1958; Fu 1981) as follows:

$$\frac{AET}{P} = 1 + \frac{PET}{P} - \left(1 + \left(\frac{PET}{P}\right)^{\omega}\right)^{(1/\omega)} \tag{3}$$

The parameter "ω" accounts for the effects of climate variability and basin characteristics such as soil, vegetation, and terrain (Donohue et al., 2007). The original

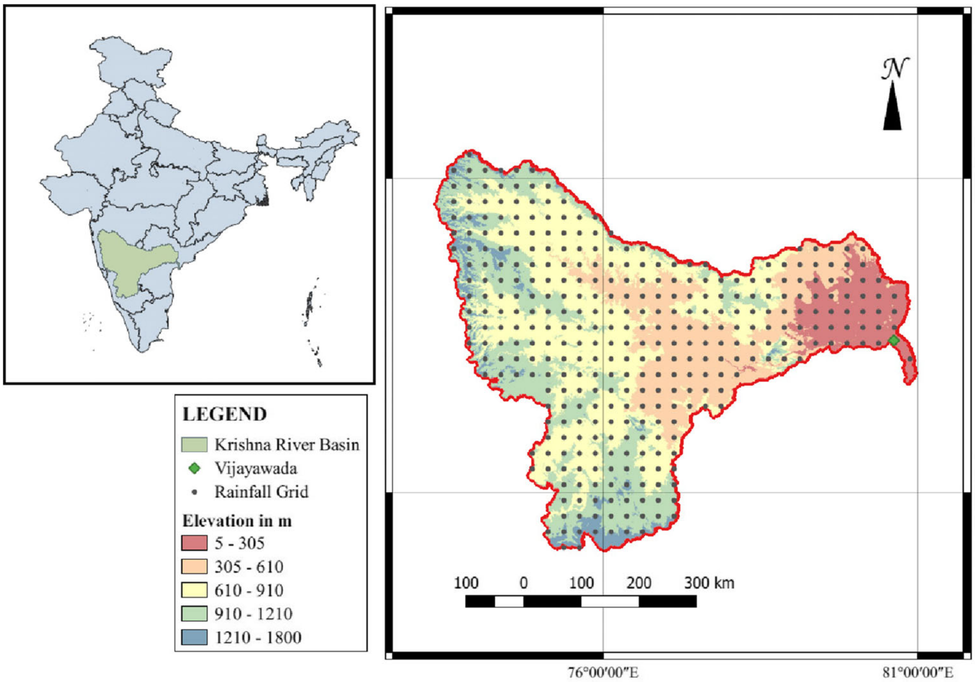
LEGEND
Krishna River Basin
Vijayawada
Rainfall Grid
Elevation in m
5 - 305
305 - 610
610 - 910
910 - 1210
1210 - 1800
N
100 0 100 200 300 km
19°00'00"N
14°00'00"N
76°00'00"E
81°00'00"E

(a)

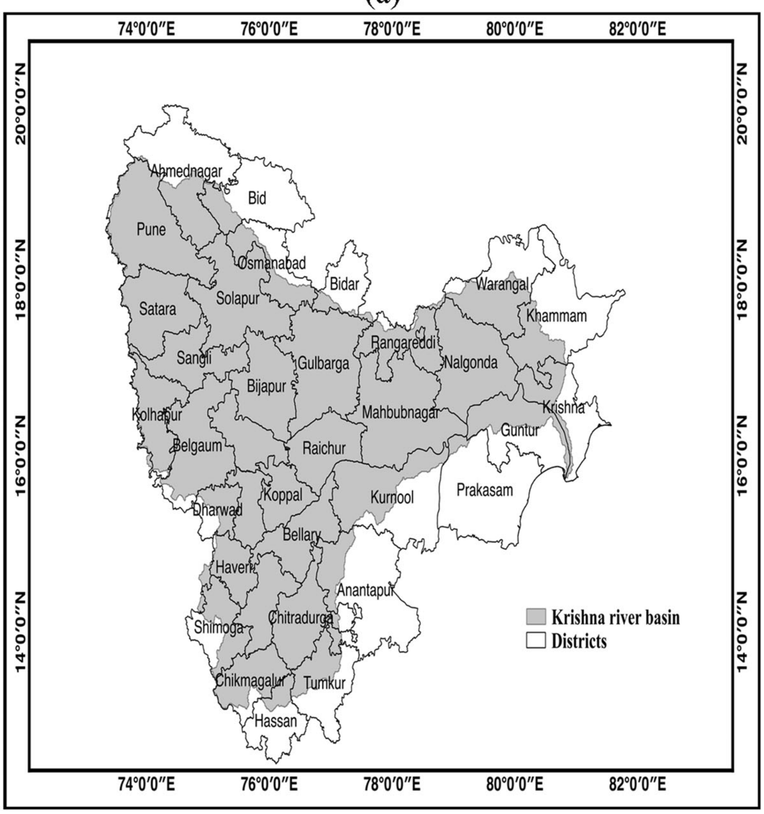
74°0'0"E
76°0'0"E
78°0'0"E
80°0'0"E
82°0'0"E
20°0'0"N
18°0'0"N
16°0'0"N
14°0'0"N
Ahmednagar
Bid
Pune
Osmanabad
Bidar
Warangal
Satara
Solapur
Khammam
Rangareddi
Sangli
Gulbarga
Nalgonda
Bijapur
Kolhapur
Mahbubnagar
Krishna
Guntur
Belgaum
Raichur
Prakasam
Kurnool
Dharwad
Koppal
Bellary
Haveri
Anantapur
Shimoga
Chitradurga
Chikmagalur
Tumkur
Hassan
Krishna river basin
Districts

(b)

Fig. 1 Map for the Krishna River basin (KRB). **a** Location of the catchment in India showing rainfall grids and basin outlet discharge gauge station at Vijayawada and elevation map superimposed on the basin. **b** Krishna basin and districts map

Budyko equation (Eq. 3) has been developed for a long-time scale (e.g., Budyko, 1974; Zhou et al., 2015). However, the Budyko framework can be applied over short periods and at annual scales (e.g., Zhang et al., 2008; Buytaert and Bièvre, 2012; Liu et al., 2017), if the parameter "ω," which represents the joint effect of climate and land surface is estimated. The present study used Budyko equation as implemented by Zhang et al. (2004) for estimating the *AET*, given as follows:

$$AET_{Budyko} = \left[P\left(1 - \exp\left(\frac{-PET}{P}\right)\right)PET\tanh\left(\frac{P}{PET}\right)\right]^{0.5} \quad (4)$$

where P, PET, and AET are at the monthly scales in millimeters. As the study intended to compare a standard *PET*-based drought indices (*SPEI*) with the proposed empirical *AET* and remote sensing ET-based drought indices, the study followed the formulation of *SPEI*. Therefore, Thornthwaite model (explained in the "Estimation of potential evapotranspiration" section) can be adopted for the estimation of monthly *PET* as per the original structure of *SPEI* (Vicente-Serrano et al. 2015). The monthly precipitation and *PET* estimated based on Thornthwaite model at monthly scales and were aggregated as given as follows:

$$P_i^k = \sum_{j=i-k+1}^{i} P_j where \ \ k = 6, 12, 18, 24 \quad (5)$$

$$PET_i^k = \sum_{j=i-k+1}^{i} PET_j \ \ where \ \ k = 6, 12, 18, 24 \quad (6)$$

where P_i^k and PET_i^k are the accumulated precipitation (in mm) and *PET* (in mm) in month i, and for various accumulation time periods of k.

AET estimation based on Turc model

Another *AET* model which also considers precipitation and *PET* and accounting for the soil and vegetative characteristics implicitly is Turc model (Turc, 1954). It is also one of the widely used *AET* models in the hydrological applications (e.g., Shibuo et al., 2007; Asokan et al., 2010; JarsjÖet al., 2004). The Turc model estimates the annual *AET* (mm) by using accumulated precipitation (Eq. 5) and *PET* (Eq. 6) in millimeters as follows:

$$AET_{Turc} = \frac{P}{\sqrt{0.9 + \frac{P^2}{PET^2}}} \quad (7)$$

The study used Budyko hypothesis and Turc models to estimate *AET*, which works at annual scale with a reasonable assumption of storage changes can be considered as constant (Gentine et al., 2012). It should be noted that, if the water balances were estimated at monthly scale, then the assumption of constant storage changes is no longer valid (Wang and Tang, 2014). Therefore, parametric formulations of Budyko (w = 0.5 in Eq. 4) and Turc (0.9 in Eq. 7) have to be tested for the applicability of the model for the river basin under consideration. The observed ET, which can be estimated with catchment scale water-balance equation, ET = precipitation (P) − runoff (R), has been compared with the *AET* estimated with parametric formulation of Budyko and Turc models. The study used Nash-Sutcliffe efficiency (NSE) and root mean square error (*RMSE*) values as performance measures in the comparison of modeled *AET* (Budyko and Turc) and observed *AET* estimates over KRB.

Estimation of potential evapotranspiration

The *PET* can be estimated based on Thornthwaite (1948) model, which considers the monthly average air temperature and geographical location of the region of interest as input variables as follows:

$$PET = 16k\left(\frac{10T}{I}\right)^a \quad (8)$$

where T is the mean monthly temperature (°C), I is the heat index (Eq. 10), and a is the location dependent coefficient (Eq. 11):

$$I = \sum_{j=1}^{12}\left[\frac{T_j}{5}\right]^{1.5} \quad (9)$$

where T_j is the mean monthly temperature during the month j (°C) for the location of interest.

$$a = 6.75 \times 10^{-7}I^3 - 7.7 \times 10^{-5}I^2 + 1.8 \times 10^{-2}I + 0.49 \quad (10)$$

I (heat index) and a (location dependent coefficient) have the same units as temperature (°C). K is the correction coefficient depending on the latitude and month, given as follows:

$$k = \left(\frac{N}{12}\right)\left(\frac{NDM}{30}\right) \quad (11)$$

where NDM is the number of days of the month and N is the maximum number of sun hours (Eq. 13) as follows:

$$N = \left(\frac{24}{\pi}\right)\varpi_s \quad (12)$$

where ϖ_s is the hourly angle of sun rising, which can be calculated as follows:

$$\varpi_s = \arccos(-\tan\phi\tan\delta) \quad (13)$$

where ϕ is the latitude in radians. If δ is the solar declination, in radians and J is the average Julian day of the month, then δ can be estimated as follows:

$$\delta = 0.4093 sen\left(\frac{2\pi J}{365} - 1.405\right) \quad (14)$$

Standardized Precipitation Evapotranspiration Index

The drought index, *SPEI* is based on the climatic water balance, the accumulated monthly difference (in mm) between precipitation and *PET* as follows:

$$D = P - PET \quad (15)$$

where P is the monthly precipitation (mm) and PET is the monthly potential evapotranspiration (mm). The estimated D values represent the water demand or surplus ($P-PET$), while the evapotranspiration is the result of complex relationship between atmosphere and surface water available, vegetation, and soil characteristics (Brutsaert, 1982). The present study adopted the structure of *SPEI* to produce standardized drought indices with three-parameter log-logistic distribution to fit the D (Eq. 15) and RAW(Eq. 2) series following to Vicente-Serrano et al. (2010). The probability density function (pdf) ($f(x)$) and cumulative distribution function (CDF) ($f(x)$) of the three-parameter log-logistic distribution are given as follows:

$$f(x) = \frac{\beta}{\alpha}\left(\frac{X-\gamma}{\alpha}\right)^{\beta-1}\left[1+\left(\frac{X-\gamma}{\alpha}\right)^{\beta}\right]^{-2} \quad (16)$$

where α, β, and γ are the scale, shape and origin parameters respectively, for D and RAW values in the range of ($\gamma > D$, $RAW < \infty$). The parameters of the log-logistic distribution are obtained by following the L-moment procedure as follows:

$$\beta = \frac{2w_1 - w_0}{6w_1 - w_0 - 6w_2} \quad (17)$$

$$\alpha = \frac{(w_0 - 2w_1)\beta}{\Gamma(1+1/\beta)\Gamma(1-1/\beta)} \quad (18)$$

$$\gamma = w_0 - \alpha\Gamma(1+1/\beta)\Gamma(1-1/\beta) \quad (19)$$

where w_0, w_1, and w_2 are the probability weighted moments calculated based on Sheng and Hashino (2007), as follows:

$$W_r = \frac{1}{n}\binom{n-1}{r}^{-1}\sum_{j=1}^{n-r}\binom{n-j}{r}x_j r = 0, 1, 2 \quad (20)$$

where n is the sample size and x_j is the ordered vector of observations in descending order. Next, the cumulative distribution function of log-logistic distribution can be calculated with the estimated parameters of Pearson-III distribution.

$$F(x) = \left[1+\left(\frac{X-\gamma}{\alpha}\right)^{-\beta}\right]^{-1} \quad (21)$$

The three-parameter log-logistic distribution was applied to model the time series of ($P-PET$) and ($P-AET$) for various time scales. Furthermore, the fitted three parameter log-logistic distribution is validated with the Kolmogorov-Smirnov (K-S) (Chakravarty et al. 1967) goodness of fit test for both the climatic water balance time series of D and RAW. A rejection frequency was defined as the ratio of number of grid points which did not fit the time series of D and RAW for log-logistic distribution, to the total number of grid points in the river basin at a given significance level (Monish and Rehana 2020).

With the values of $F(x)$ (Eq. 21), the *SPEI* values were calculated as follows:

$$SPEI = W - \frac{C_0 + C_1 W + C_2 W^2}{1 + d_1 W + d_2 W^2 + d_3 W^3} \quad (22)$$

where $W = \sqrt{-2\ln(p)}$ for $P \le 0.5$ (23)

where P is the probability of exceeding a determined D value, $P = 1 - F(x)$. If $P > 0.5$, then P is replaced by $1-P$ and the sign of the resultant *SPEI* is reversed. The constants are C0 = 2.5515517, C1 = 0.802583, C2 = 0.010328, d1 = 1.432788, d2 = 0.189269, and d3 = 0.001308, by substituting the C0, C1, and C2 values in Eq. 22. The drought severity of SPEI/$SPAEI_{Budyko}$/$SPAEI_{Turc}$/$SPAEI_{RS\_ET}$ can be identified based on Vicente-Serrano et al. (2010) categorization as follows: moderate if SPEI/$SPAEI_{Budyko}$/$SPAEI_{Turc}$/$SPAEI_{RS\_ET}$ were in between − 1.0 and − 1.49, severe if SPEI/$SPAEI_{Budyko}$/$SPAEI_{Turc}$/$SPAEI_{RS\_ET}$ were in between − 1.50 and − 1.99, and extreme if SPEI/$SPAEI_{Budyko}$/$SPAEI_{Turc}$/$SPAEI_{RS\_ET}$ were less than − 2.0.

The Standardized Precipitation-Actual Evapotranspiration Index (SPAEI) can account for the hydrological drought also to some extent because it considers actual evapotranspiration as it is defined as a function of major hydrological variables (i.e., *P*, *PET*, and *AET*). Generally, *SPEI* can be expressed at different time scales as *SPEI* (6), *SPEI* (12), etc., where the number in the bracket indicates the timescale in months for which the *P*−*PET* values are accumulated and the estimated *SPEI* at these timescales. The present study used the drought indices as 6-, 12-, 18-, and 24-month accumulation time periods for the drought characterization over the river basin. The ability of *SPEI* and various formulations of SPAEI to reproduce drought conditions has been compared at a river basin scale of Krishna River, India.

Data used in the study

The gridded daily precipitation data from the India Meteorological Department (IMD) available for the period of 1901 to 2015 at 0.25° × 0.25° resolution was used as precipitation observational dataset (Rajeevan and Bhate, 2009). The gridded daily average temperature at a resolution of 1° × 1° for the period of 1951–2014 was used as temperature observational data sets (Srivastava et al., 2009). More details about the data are available from http://www.imd.gov.in/advertisements/20170320_advt_34.pdf. The daily temperature data was interpolated to 0.25° × 0.25° resolution using the inverse distance weighting method. The daily gridded precipitation and temperature data at 0.25° × 0.25° resolution available over the Indian land mass were cropped for KRB. About 348 grid points encompassing the entire basin were considered in the drought analysis. The daily precipitation and temperatures data sets obtained from IMD were aggregated over monthly time scale to serve as primary inputs to calculate *SPEI*, $SPAEI_{Budyko}$, and $SPAEI_{Turc}$ at each grid at 0.25° × 0.25° resolution. The average monthly air temperature data sets were used in the estimation of *PET* using Thornthwaite model. Further, the estimated monthly *PET* and *P* were forced in the AET_{Budyko} and AET_{Turc} models to estimate the *SPEI*, $SPAEI_{Budyko}$, and $SPAEI_{Turc}$ drought indices. A common data period of 1951 to 2014 was considered for the drought analysis, over KRB to understand the climate and drought variability.

Further, to study the strength of the proposed *AET*-based drought indices ($SPAEI_{Budyko}$, $SPAEI_{Turc}$) in predicting the drought characteristics, the present study used satellite-based land surface *ET* estimates. In the present study, satellite-based land surface global *ET* product derived from the Numerical Terradynamic Simulation Group (http://files.ntsg.umt.edu/data/ET_global_monthly_ORIG/Global_HalfDegResolution), from 1983 to 2006 at 0.5° × 0.5° resolution was adopted. The continuous satellite-derived global land surface *ET* was developed based on Moderate Resolution Imaging Spectroradiometer (MODIS) data, meteorological observations, and satellite-based vegetation parameters. The *ET* data accounts for the canopy transpiration and soil evaporation with modified Penman-Monteith approach, biome-specific canopy conductance from Normalized Difference Vegetation Index (NDVI), and open water evaporation from Priestley-Taylor approach (Zhang et al., 2010), which was found in general agreement with most of the global basins (Liu et al., 2016). The original land surface satellite-based *ET* data was at 0.5° × 0.5° resolution which was rescaled to 0.25° × 0.25° resolution by bilinear spatial interpolation method.

Results and discussions

The present study compared the *AET* estimated with Budyko (Eq. 4) and Turc (Eq. 7) models at basin averaged annual scale with observed *AET* estimated with water balance equation as shown in Fig. 2. On the basin scale, the modeled *AET* values of Budyko and Turc yielded a bias of 51.1 and 38.4 respectively in comparison with water balance–based *AET*. The NSE values estimated between observed and Budyko and Turc modeled *AET* estimates were noted as 0.63 and 0.74 respectively, whereas the *RMSE* values estimated between observed and Budyko and Turc modeled *AET* estimates were obtained as 87 and 74 respectively. With this, the parametric formulations of *AET* was

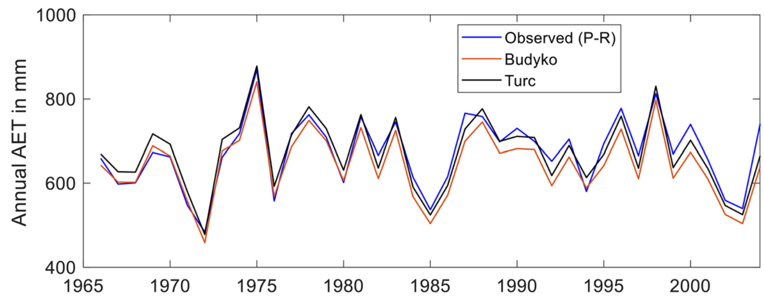

Fig. 2 Comparison of observed basin averaged annual estimates of *AET* from *ET* = *P*−*R* with Budyko and Turc model estimates

identified as reliable measures to estimate *AET* over KRB. However, applicability of annual scale *AET* models in the short-term scale monthly drought assessment is always debatable question (Wang and Tang, 2014), but the present study made efforts to test the success of implication of such catchment scale annual *AET* models in the drought assessment at regional scales.

The K-S rejection frequencies with three-parameter log-logistic distribution for the overall basin including all valid grid points were obtained as 6%, 8%, and 7.7% for *SPEI*, $\mathrm{SPAEI}_{\mathrm{Budyko}}$, and $\mathrm{SPAEI}_{\mathrm{Turc}}$ respectively at a significance level of 0.01. To assess *SPEI* and SPAEI, for meteorological drought detection, the years when the annual precipitation is less than 75% of the annual average estimated over a period of 1951 to 2014 were considered based on the IMD definition of drought year (http://imd.gov.in/section/nhac/wxfaq.pdf). Four drought years were identified based on the deviation of annual precipitation from the normal precipitation of the period 1951–2014. Based on Fig. 3 (a), these drought years have been identified as 1972, 1985, 2002, and 2003. These drought years are among the major documented drought events over Indian monsoon region (De et al., 2005; Mallya et al., 2016). Among these, the 2002 was one of the severe drought years in India, which has affected 56% of its geographical area, livelihoods of 300 million people (https://public.wmo.int/en/bulletin/flood-and-drought-management-through-water-resources-development-india). Furthermore, the drought years over the basin as identified in the present study were also agreeable with the study of Sinha et al. (2019), in which the period July 2002 to June 2005 was identified as longest drought period. Therefore, various drought indices of *SPEI* and SPAEI based on empirical models were studied for the drought affected years of 1972, 1985, 2002, and 2003 over KRB in terms of areal extent, severity, frequency, and duration. Furthermore, as the satellite-based *ET* data used in the estimation of drought indices considered the surface energy balances, *ET* from vegetated areas, evaporation from water bodies, biome-specific NDVI-derived canopy conductance in the *ET* estimation (Zhang et al., 2010), the study considered the drought indices estimated based on such data as a base for the comparison of empirical *AET*-based drought indices (Shah and Mishra, 2015). The present study compared various drought characteristics estimated based on empirical *AET* models with remote sensing-ET (RS-ET) data for the drought affected years of the basin.

To study the spatial drought characterization, the areal extent of droughts represented as percentage of grids for moderate ($-1 \le \mathrm{SPEI}/\mathrm{SPAEI}_{\mathrm{Budyko}}/\mathrm{SPAEI}_{\mathrm{Turc}}/\mathrm{SPAEI}_{\mathrm{RS\text{-}ET}} \le -1.49$), severe ($-1.5 \le \mathrm{SPEI}/\mathrm{SPAEI}_{\mathrm{Budyko}}/\mathrm{SPAEI}_{\mathrm{Turc}}/\mathrm{SPAEI}_{\mathrm{RS\text{-}ET}} \le -1.99$), and extreme ($\mathrm{SPEI}/\mathrm{SPAEI}_{\mathrm{Budyko}}/\mathrm{SPAEI}_{\mathrm{Turc}}/\mathrm{SPAEI}_{\mathrm{RS\text{-}ET}} < -2$) was studied out of total number of 348 grid points over the basin at 12-month time scale (Fig. 3, Table 1). The percentages of annual moderate and severe drought affected areas were observed to be increasing over KRB for the period of 1951–2014 with all drought indices under consideration. The areal extents of moderate, severe, and extreme droughts were observed to be more for the drought years of 1972, 1985, 2002, and 2003 with all four drought indices. The remote sensing-based drought index, $\mathrm{SPAEI}_{\mathrm{RS\text{-}ET}}$, also identified the years 1985, 2002, and 2003 as highly affected drought years in terms of higher percentage of areal extent for moderate, severe, and extreme categories of droughts for the period of 1983 to 2006. The percentage of drought areal extents with *SPEI*, $\mathrm{SPAEI}_{\mathrm{Budyko}}$, $\mathrm{SPAEI}_{\mathrm{Turc}}$, and $\mathrm{SPAEI}_{\mathrm{RS\text{-}ET}}$ for various categories of droughts were studied for the major drought years over the basin (Table 1). The moderate drought areal extents with empirical *AET*-based drought indices ($\mathrm{SPAEI}_{\mathrm{Budyko}}$ and $\mathrm{SPAEI}_{\mathrm{Turc}}$) were observed to be more compared to *SPEI* (Fig. 3(b), Table 1). However, the percentage of the severe and extreme drought areas were noted to be higher with *SPEI* compared to both $\mathrm{SPAEI}_{\mathrm{Budyko}}$ and $\mathrm{SPAEI}_{\mathrm{Turc}}$ (Fig. 3(c), Table 1).

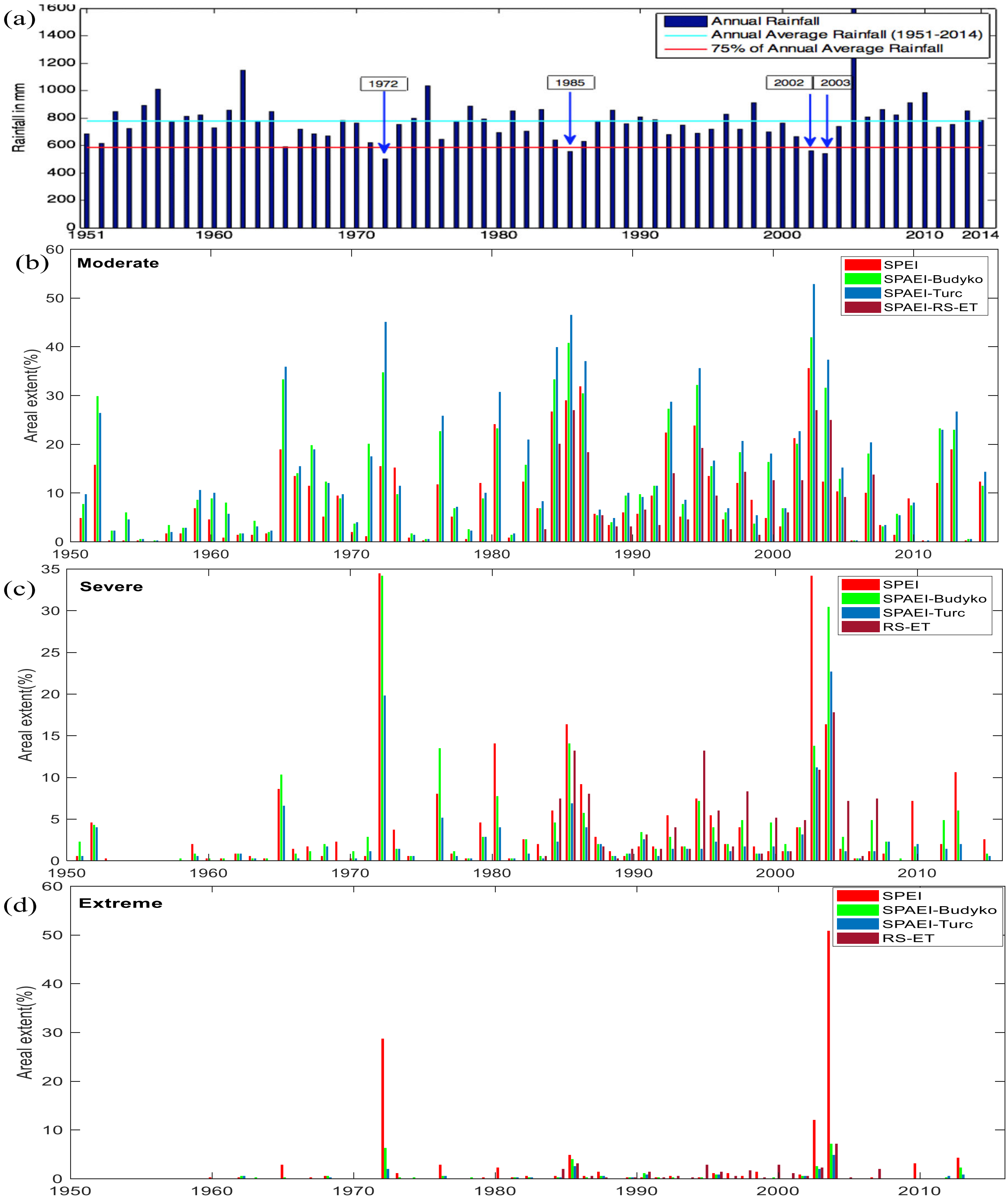

Fig. 3 **a** Annual precipitation of Krishna River basin compared to long-term average annual precipitation. **b** Areal extent of moderate droughts represented as percentage of grids with *SPEI* and SPAEI < − 1 at 12-month time window. **c** Areal extent of severe droughts represented as percentage of grids with *SPEI* and SPAEI < − 2 at 12-month time window

Table 1 Drought area in Krishna basin based on *SPEI*, $SPAEI_{Budyko}$, $SPAEI_{Turc}$, and $SPAEI_{RS\text{-}ET}$

Year	Drought type	*SPEI*	$SPAEI_{Budyko}$	$SPAEI_{Turc}$	$SPAEI_{RS\text{-}ET}$
1972	Moderate	16.00	34.40	44.27	*
	Severe	33.33	33.33	19.47	*
	Extreme	28.53	6.67	2.40	*
1985	Moderate	28.80	39.73	45.87	27.01
	Severe	15.73	14.13	7.20	13.22
	Extreme	4.53	3.73	2.40	3.16
2002	Moderate	35.20	42.93	52.80	27.01
	Severe	35.47	13.87	11.73	10.92
	Extreme	11.47	2.40	1.87	2.30
2003	Moderate	13.60	31.20	36.53	25
	Severe	16.27	28.80	21.60	17.82
	Extreme	49.07	7.20	5.07	7.18

*Data unavailable

As *SPEI* consider the residual water available for evaporation based on energy available, in terms of *PET*, higher severe and extreme drought areal extents were estimated. While *AET*-based drought indices account for the residual available water for evaporation based on both energy and water, moderate drought percentage areal extents were noted compared to *SPEI*. For example, for the recent consecutive drought years of 2002 and 2003, about 11.47%, 2.4%, 1.87%, 2.3%, and 49.07%, 7.2%, 5.07%, 7.2% of the river basin was noted under extreme with *SPEI*, $SPAEI_{Budyko}$, $SPAEI_{Turc}$, and $SPAEI_{RS\text{-}ET}$ respectively. Furthermore, $SPAEI_{Budyko}$ indices were identified as a more reliable measure in the estimation of drought areal extent by comparing with satellite-based land surface *ET* data ($SPAEI_{RS\text{-}ET}$), while the Turc model has under predicted the extreme drought areal extents compared to $SPAEI_{Budyko}$ and $SPAEI_{RS\text{-}ET}$. Furthermore, to support such research findings, the spatial drought characterizations for the major drought years of 1972, 1985, 2002, and 2003 were presented in Fig. 4. The years 1972 and 2003 were noted as most severe historic droughts occurred over KRB as most of the basin was classified under extreme drought. For the 1972 drought year, the upper portion of the basin, particularly, Maharashtra, North Karnataka, and Telangana, was classified under extreme drought regions with *SPEI*, whereas *AET*-based drought indices have noted few districts into moderate. Such noticeable deviation in the drought categorization from extreme/severe to moderate can also be seen for the drought years of 2002 and 2003. Therefore, the driving of areal extents between *SPEI* and SPAEI for severe and extreme droughts is more evident, then the moderate drought areal extents. For drought years of 1985, 2002, and 2003, the severe and extreme drought extents with $SPAEI_{Budyko}$ and $SPAEI_{Turc}$ were found to be the more comparable with $SPAEI_{RS\text{-}ET}$ than with *SPEI* (Table 1). Thus, *PET*-based drought indices categorize more percentage of area as severe or extreme, which were identified as moderate drought areas otherwise with *AET*-based drought indices.

The *PET*- and *AET*-based drought indices were compared in terms of drought intensity for 12-month accumulation periods as shown in Fig. 5. The drought severity for major droughts for 12-month accumulated time period was compared for four drought indices as given in Table 2. The *SPEI* is able to reconstruct most of the drought years as moderate and severe, whereas SPAEI-based drought indices have recognized them as mild drought years. The SPAEI formulations of empirical and remote sensing-based drought indices were identified the major droughts as less intensified compared to *SPEI*. For example, the *SPEI*-12, $SPAEI_{Budyko}$-12, $SPAEI_{Turc}$-12, and $SPAEI_{RS\text{-}ET}$-12 values for the drought years of 2002 and 2003 were obtained as − 1.43, − 1.06, − 1.10, − 0.83 and − 1.80, − 1.15, − 1.06, − 0.88 respectively. Overall, the severities of the drought indices were found to be more with *SPEI* compared to $SPAEI_{Budyko}$, $SPAEI_{Turc}$, and $SPAEI_{RS\text{-}ET}$. Therefore, the present study revealed that inclusion of *AET* in the drought assessment characterize the droughts as moderately intensified which were otherwise identified as severe droughts with *PET*-based drought indices.

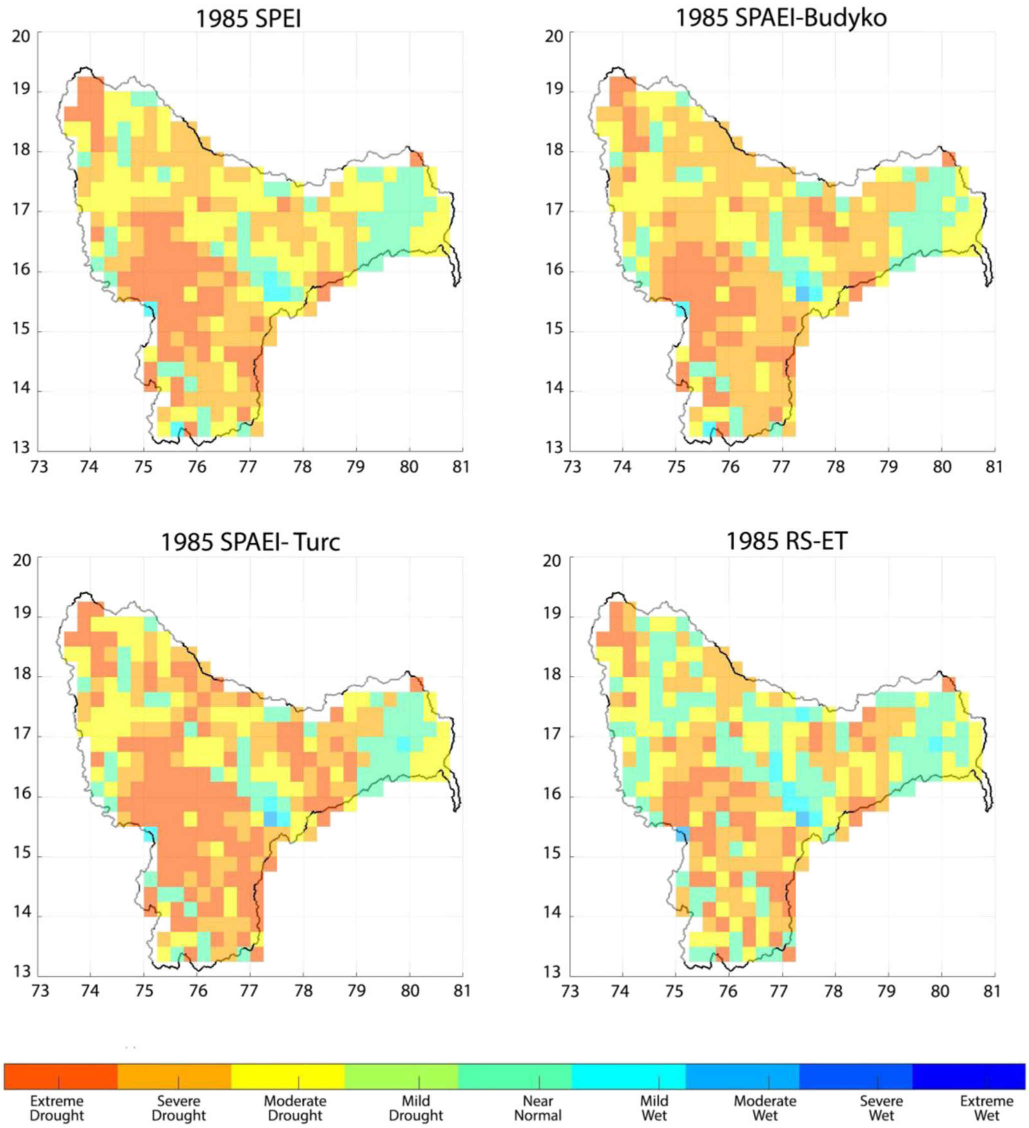

Fig. 4 Spatial drought categorizations based on *SPEI*, $SPAEI_{Budyko}$, $SPAEI_{Turc}$, and remote sensing *ET* at 12-month scale over Krishna River basin for drought years of 1985, 2002, and 2003

Further, drought severities were noted to be less with $SPAEI_{Turc}$ compared to $SPAEI_{Budyko}$ due to the lower estimates of *AET* with Turc model, representing the dependence of severity or intensity of droughts on the quantification of *AET* estimates. Also, the $SPAEI_{RS\text{-}ET}$-12 was not able to detect the major drought years of the basin, due to the less magnitude of *AET* estimates compared to the Budyko and Turc modeled *AET* estimates. The basin average *AET* estimates for observed, Budyko, Turc, and remote sensing were noted as 710.4, 662.35, 689.82, and 505.7 mm respectively. Therefore, the drought intensities are defined more by *ET* compared to the precipitation over an arid region. Overall, there exists a strong influence on drought severities with the use of various formulations of *ET* estimates in drought characterization over an arid river basin.

Figure 6 shows the comparison of severe and extreme drought frequencies (SPEI/$SPAEI_{Budyko}$)/

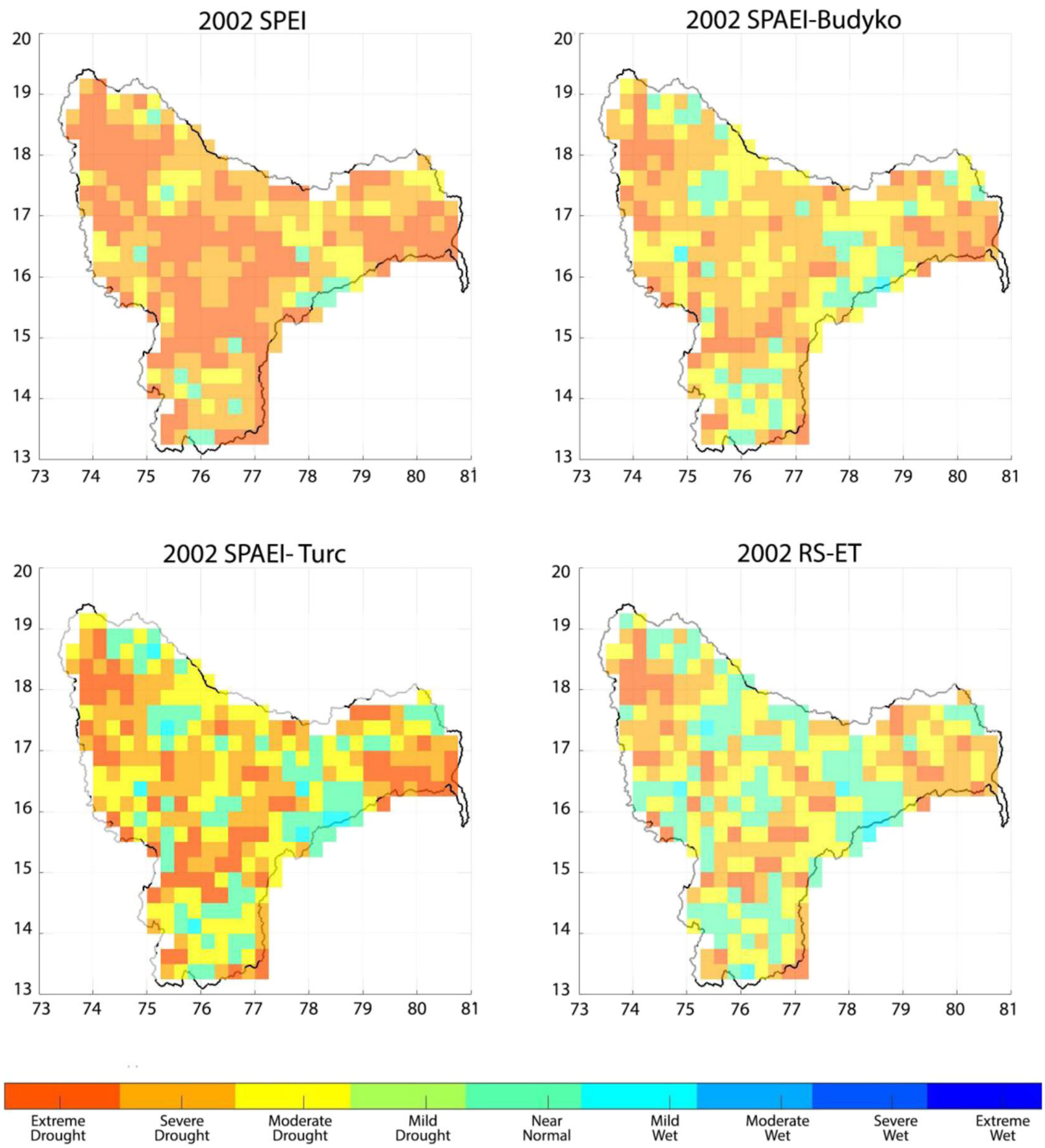

Fig. 4 (continued)

$SPAEI_{TURC}/SPAEI_{RS\text{-}ET} > -1.50$) over Krishna River basin for 1983–2006. The *PET*-based drought index (*SPEI*) has resulted in higher drought frequencies for the period of 1983–2006 compared to both empirical based *AET* ($SPAEI_{Budyko}$ and $SPAEI_{Turc}$) and remote sensing-based ($SPAEI_{RS\text{-}ET}$) drought indices over KRB. The remote sensing-based severe and extreme drought frequencies were more comparable with Budyko model drought frequencies for the river basin for the period of 1983–2006.

The present study considered a threshold of − 1 for both *SPEI* and SPAEI formulations in drought duration estimation. The drought duration was identified as the period of months which is continuous negative, started from the $SPEI/SPAEI_{Budyko}/SPAEI_{Turc}/SPAEI_{RS\text{-}ET}$ values are more than − 1 and ends when the $SPEI/SPAEI_{Budyko}/SPAEI_{Turc}/SPAEI_{RS\text{-}ET}$ values turns out to be positive. The duration and intensities of droughts were studied for the recent two consecutive drought years of 2002 and 2003 over

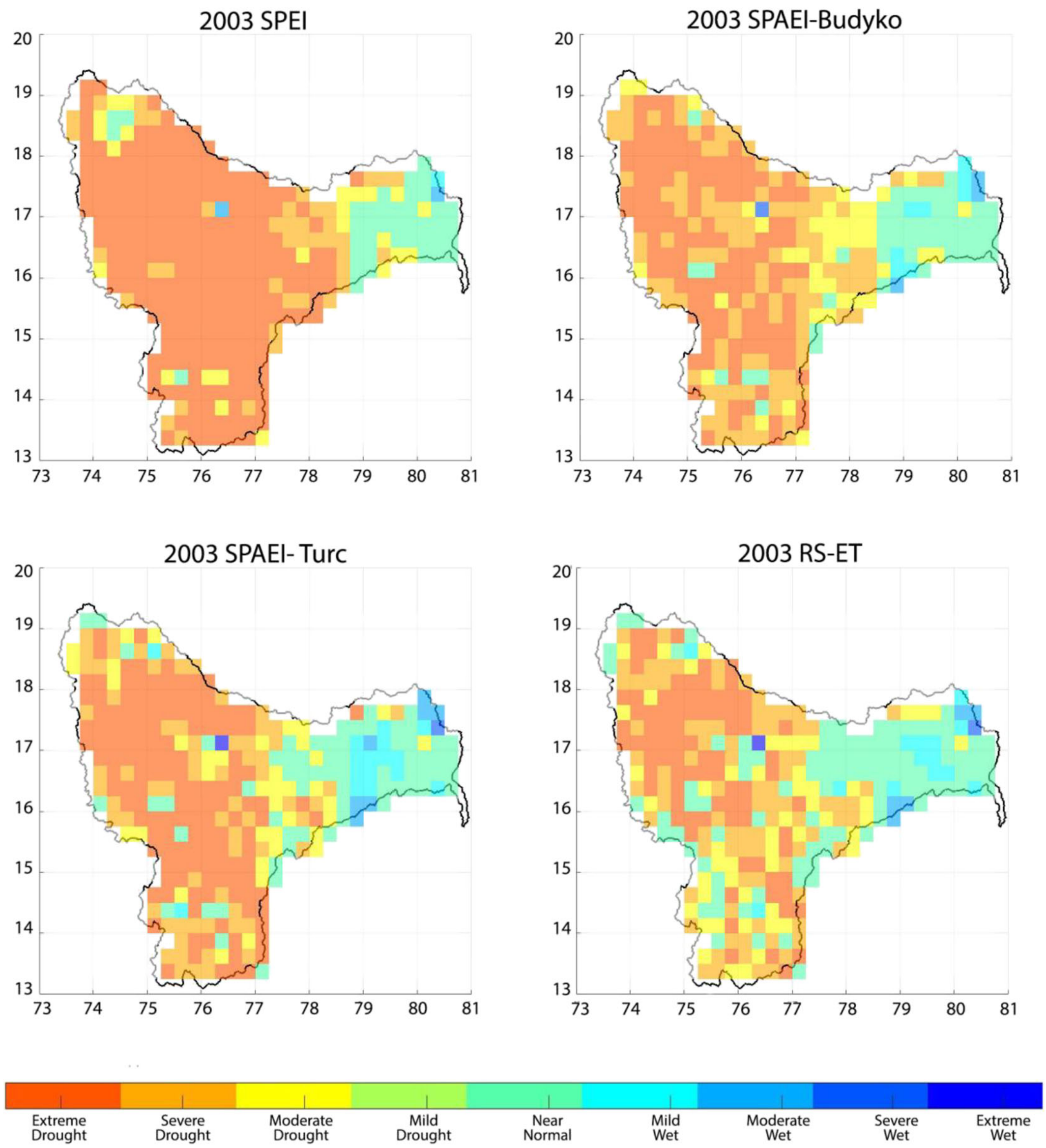

Fig. 4 (continued)

the river basin for 6-, 12-, 18-, and 24-month scales (Fig. 7). The *SPEI* at 6-month drought duration was noted as from May to August and May to September for year 2002 and 2003 respectively with intensity as moderate, whereas the $\mathrm{SPAEI}_{\mathrm{Budyko\text{-}6}}$ and $\mathrm{SPAEI}_{\mathrm{Turc\text{-}6}}$ have identified 2002 and 2003 as normal conditions from March to September and February to September respectively and the $\mathrm{SPAEI}_{\mathrm{RS\text{-}ET}}$ at 6-month time scale has identified the drought duration as April for 2002 and 2003 years. Similarly, SPEI12 duration of moderate drought months was noted from September 2002 to December 2003, whereas $\mathrm{SPAEI}_{\mathrm{Budyko}}$ and $\mathrm{SPAEI}_{\mathrm{Turc}}$ have identified May and June 2003 as major drought affected months. The $\mathrm{SPAEI}_{\mathrm{RS\text{-}ET}}$ at 12-month scale has estimated the drought duration as June 2003. Similarly, such short and less intensified droughts were noted also with 18- and 24-month time scale of the drought indices. Further, the empirical based *AET* drought indices and remote sensing–based *ET* drought index has shown comparable drought durations at

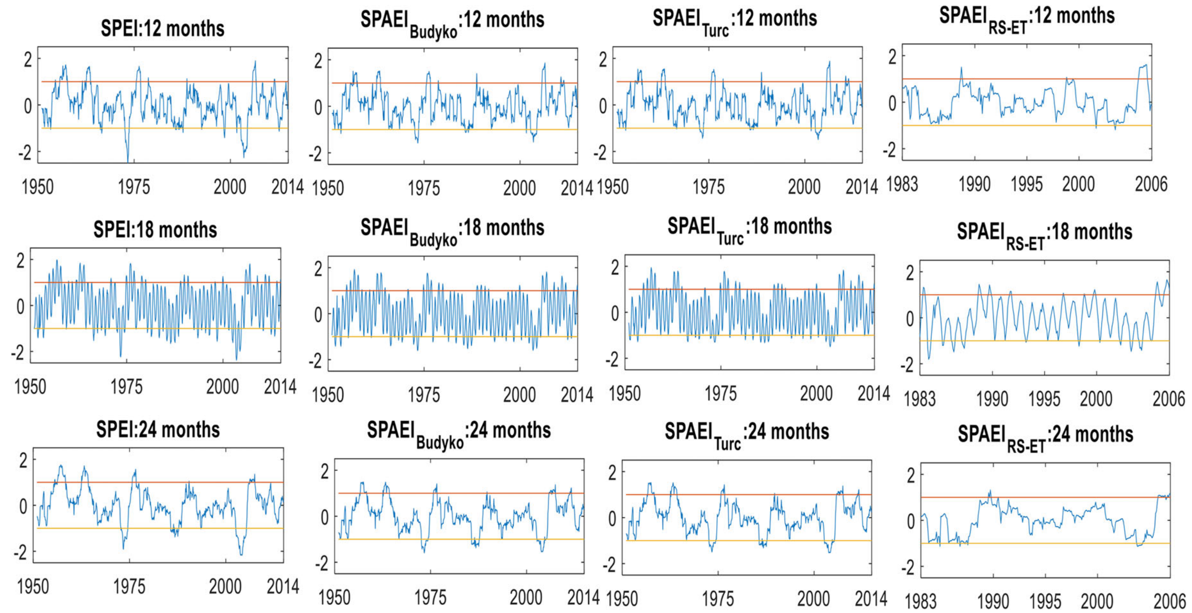

Fig. 5 Time series of *SPEI*, $\mathrm{SPAEI_{Budyko}}$, $\mathrm{SPAEI_{Turc}}$, and $\mathrm{SPAEI_{RS\text{-}ET}}$ for different accumulated periods of 12, 18, and 24 months for the period of 1951 to 2014 over Krishna River basin

Table 2 Drought intensity for major drought years of 1972, 1985, 2002, and 2003 drought years as estimated by *SPEI*, $\mathrm{SPAEI_{Budyko}}$, $\mathrm{SPAEI_{Turc}}$, and remote sensing *ET* over Krishna River basin

Year	*SPEI*	$\mathrm{SPAEI_{Budyko}}$	$\mathrm{SPAEI_{Turc}}$	$\mathrm{SPAEI_{RS\text{-}ET}}$
6-month scale				
1972	− 1.42	− 0.69	− 0.77	*
1985	− 1.40	− 0.98	− 0.74	− 0.30
2002	− 1.57	− 0.85	− 1.01	− 0.42
2003	− 2.00	− 0.97	− 0.81	− 0.23
12-month scale				
1972	− 1.51	− 1.24	− 1.05	*
1985	− 0.98	− 1.03	− 0.98	− 0.86
2002	− 1.43	− 1.06	− 1.10	− 0.83
2003	− 1.80	− 1.15	− 1.06	− 0.88
18-month scale				
1972	− 2.07	− 1.33	− 1.20	*
1985	− 1.46	− 1.21	− 1.19	− 0.39
2002	− 2.21	− 1.40	− 1.38	− 0.18
2003	− 1.76	− 1.15	− 1.15	− 0.89
24-month scale				
1972	− 1.77	− 1.40	− 1.35	*
1985	− 1.08	− 1.14	− 1.11	− 0.89
2002	− 1.26	− 0.99	− 1.03	− 0.77
2003	− 1.99	− 1.42	− 1.40	− 1.09

*Data unavailable

various accumulation periods. Overall, short drought durations were noticed with both *AET*-based drought indices compared to *PET*-based drought index.

Summary and discussion

The hypothesis of use of climatic water balance based on *AET* in the drought characterization will drive the extreme drought characterization into moderate was tested in terms of severity, spatial extent, duration, and frequency. For this, the present study developed a drought index which can combine the structure of *SPEI* and *AET*, the SPAEI. The formulation of SPAEI based on *P* −*AET* accounts for the water balance of the river basin representing the available water to fulfil the evaporation demands, where long-term storage losses are neglected. The use of *AET* in the drought estimation conceptually accounts for the soil water storage, water supply, and energy available; therefore, SPAEI can also characterize the hydrological drought conditions implicitly. The drought characterization based on two climatic water balances, one is with *PET* and other with *AET*, was compared for KRB, India. For calculating

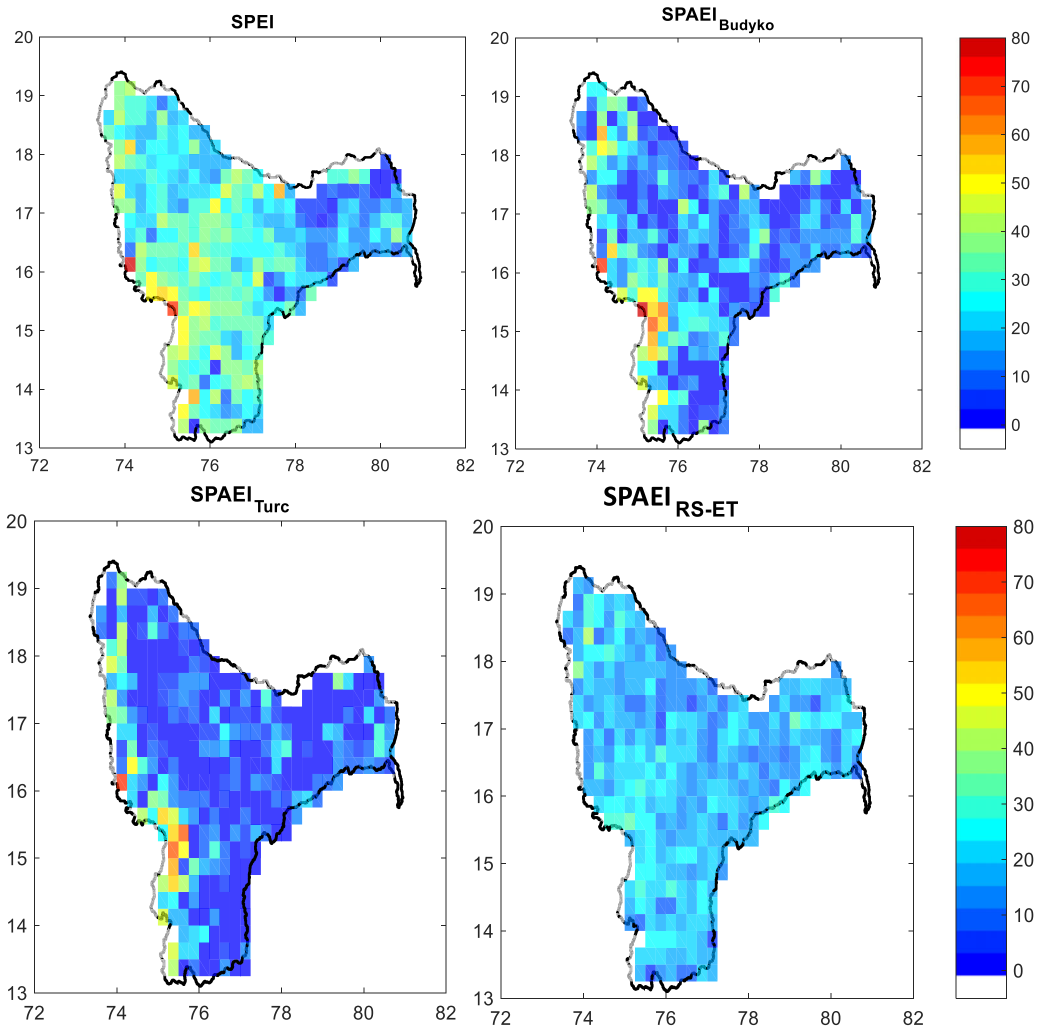

Fig. 6 Number of severe and extreme drought events (SPEI/SPAEI$_{Budyko}$)/SPAEI$_{TURC}$/SPAEI$_{RS\text{-}ET}$ > −1.50) over Krishna River basin for 1983–2006

SPEI and SPAEI at different time scales of 12, 18, and 24 months, for the period of 1951 to 2014, the monthly precipitation and temperatures at 0.25-degree resolution have been used. To validate and to assess the strength of the use of empirical *AET* estimates in the drought characterization, the results were compared with drought indices resulting from remote sensing–based *ET* estimates. The drought indices developed in the present study has revealed that inclusion of *AET* in the drought assessment will result in less intensified droughts compared with *PET*-based drought indices. The *PET*-based drought index, *SPEI*, overestimates the drought intensity as it is based on unlimited water supply and energy, whereas the SPAEI is a reliable measure as it agrees better with the natural water budget of a river basin. The *AET*-based drought indices were able to drive the areas into moderate, which or otherwise categorized under severe drought regions. Inclusion of *AET* in the drought characterization along with precipitation and *PET* can drive the highly intensified drought events determined by *SPEI* into moderate and less frequent droughts with short durations. Further, the comparison and validation of drought indices in terms of areal extent, intensity, frequency, and

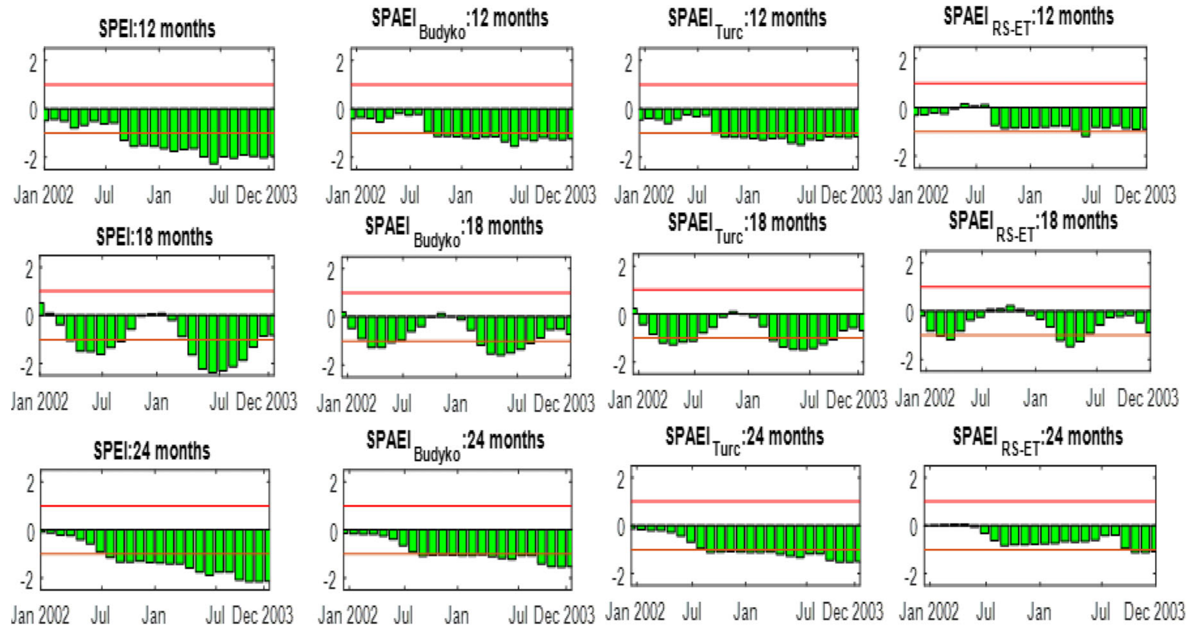

Fig. 7 Duration and intensities of drought for the drought years of 2002 and 2003 over Krishna River basin for various time scales for *SPEI* and SPAEI

duration based on Budyko- and Turc-based *AET* models have provided the sensitivity of *AET* estimates in the drought characterization. Further, the Budyko model integrated drought formulation as presented in the study is more comparable with remote sensing ET-based drought index.

Nevertheless, the proposed methodology to estimate the monthly and annual *AET* is based on Budyko hypothesis (Budyko, 1958) and the empirical equations generated by Zhang et al. (2004). The parameter which represents the basin characteristics of vegetation and climate change in the estimation of *AET* was considered as stationary. However, to consider the joint effect of climate and land surface variability, a dynamic parameter of Budyko-type formula can be applied (Liu et al., 2017). Further, employing a regional hydrological model to simulate the *AET* at river basin scale and accounting for the dynamic parameter of Budyko-type formula can be a potential future research problem. As most difficult variables to measure in the regional water balance assessment (Lettenmaier and Famiglietti, 2006) are *PET* and *AET* in addition to precipitation and streamflow, these variables deserve more attention towards estimation and understanding the variability. Given the concern of increasing droughts worldwide under climate change, evaluation of variability associated with retrospective drought events will be valuable towards the understanding of regional drought patterns. Such analysis will provide as a basis of possible future droughts and potential vulnerabilities.

Funding information The research work presented in the manuscript is funded by Science and Engineering Research Board (SERB), Department of Science and Technology, Government of India, through Start-up Grant for Young Scientists (YSS) Project no. YSS/2015/002111 to Dr. S. Rehana

Compliance with ethical standards

Conflict of interest The authors declare that they have no conflict of interest.

References

Aadhar, S., & Mishra, V. (2017). High-resolution near real-time drought monitoring in South Asia. *Scientific Data, 4*, 170145.

Allen, K. J., Ogden, J., & Buckley, B. M. (2011). The potential to reconstruct broad scale climate indices associated with southeast Australian droughts from Athrotaxis species. *Tasmania, Climate Dynamics, 37*, 1799–1821.

Asokan, S. M., Jarsjö, J., & Destouni, G. (2010). Vapor flux by evapotranspiration: effects of changes in climate, land use, and water use. *Journal of Geophysical Research-Atmospheres, 115*, D24.

Brutsaert, W.F.,1982. Evaporation into the atmosphere. D. Reidel., Norwell, Mass, 299 pp.

Budyko, M. I., 1958. The heat balance of the earth's surface. Translated by N. A. Stepanova, U.S. Dept. of Commerce, 259 pp.

Budyko, M. I., 1974. Climate and life. International Geophysical Series, Vol. 18, Academic Press, 507 pp.

Buytaert, W., & Bièvre, B. D. (2012). Water for cities: the impact of climate change and demographic growth in the tropical Andes. *Water Resources Research, 48*, W08503. https://doi.org/10.1029/2011WR011755.

Chakravarty, I. M., Roy, J. D. and Laha, R. G. 1967. Handbook of methods of applied statistics.

Cook, B. I., Smerdon, J. E., Seager, R., & Coats, S. (2014). Global warming and 21st century drying. *Climate Dynamics, 43*(9-10), 2607–2627.

Dai, A. G. (2011). Drought under global warming: a review. *Wires Climate Change., 2*(1), 45–65.

De, U. S., Dube, R. K., & Rao, P. G. S. (2005). Extreme weather events over India in the last 100 years. *Journal of Indian Geophysical Union, 9*, 173–187.

Donohue, R. J., Roderick, M. L., & McVicar, T. R. (2007). On the importance of including vegetation dynamics in Budyko's hydrological model. *Hydrology and Earth System Sciences, 11*(2), 983–995.

Fu, B. P. (1981). On the calculation of the evaporation from land surface (in Chinese). *Scientia Atmospherica Sinica, 5*, 23–31.

Gentine, P., D'Odorico, P., Lintner, B., Sivandran, G., & Salvucci, G. D. (2012). Interdependence of climate, soil, and vegetation as constrained by the Budyko curve. *Geophysical Research Letters, 39*, L19404. https://doi.org/10.1029/2012GL053492.

George, B., Malano, H., Davidson, B., Hellegers, P., Bharati, L., & Massuel, S. (2011). An integrated hydro-economic modelling framework to evaluate water allocation strategies: I. *Model development. Agric. Water Manage., 98*, 733–746.

Hayes, M., Wilhite, D. A., Svoboda, M., & Vanyarkho, O. (1999). Monitoring the 1996 drought using the standardized precipitation index. *Bull. Amer. Meteor. Soc, 80*, 429–438.

Homdee, T., Pongput, K., & Kanae, S. (2016). A comparative performance analysis of three standardized climatic drought indices in the Chi river basin, Thailand. *Agriculture and Natural Resources, 50*(3), 211–219.

Jarsjo, J., Shibuo, Y., Destouni, G., 2004. Using the PCRasterPOLFLOW approach to GIS-based modelling of coupled groundwater–surface water hydrology in the Forsmark Area. Swedish Nuclear Fuel and Waste Management Co Report R-04-54.

Kim, D., & Rhee, J. (2016). A drought index based on actual evapotranspiration from the Bouchet hypothesis. *Geophysical Research Letters, 43*(19).

Kumar, K. N., Rajeevan, M., Pai, D. S., Srivastava, A. K., & Preethi, B. (2013). On the observed variability of monsoon droughts over India. *Weather and Climate Extremes, 1*, 42–50.

Lettenmaier, D. P., & Famiglietti, J. S. (2006). Hydrology: water from on high. *Nature, 444*, 562–563.

Liu, W., Wang, L., Zhou, J., Li, Y., Sun, F., Fu, G., Li, X., & Sang, Y.-F. (2016). A worldwide evaluation of basin-scale evapotranspiration estimates against the water balance method. *Journal of Hydrology, 538*, 82–95.

Liu, M., Xu, X., Xu, C., Sun, A. Y., Wang, K., Scanlon, B. R., & Zhang, L. (2017). A new drought index that considers the joint effects of climate and land surface change. *Water Resources Research, 53*, 3262–3278.

Mallya, G., Mishra, V., Niyogi, D., Tripathi, S., & Govindaraju, R. S. (2016). Trends and variability of droughts over the Indian monsoon region. *Weather and Climate Extremes., 12*, 43–68.

McKee, T. B., Doesken, N. J., and Kleist, J., 1993. The relationship of drought frequency and duration to time scales. American Meteorological Society. 8th Conference on Applied Climatology.17(22) Janvier, Anaheim, 179-184.

Milly, P. C. D. (1994). Climate, soil water storage, and the average annual water balance. *Water Resources Research, 30*, 2143–2156.

Monish, N. T., & Rehana, S. (2020). Suitability of distributions for standard precipitation and evapotranspiration index over meteorologically homogeneous zones of India. *Journal of Earth System Science, 129*(1), 25.

Mu, Q., Zhao, M., Kimball, J. S., McDowell, N. G., & Running, S. W. (2013). A remotely sensed global terrestrial drought severity index. *Bulletin of the American Meteorological Society, 94*(1), 83–98.

Narasimhan, B., & Srinivasan, R. (2005). Development and evaluation of Soil Moisture Deficit Index (SMDI) and Evapotranspiration Deficit Index (ETDI) for agricultural drought monitoring. *Agricultural and Forest Meteorology, 133*(1-4), 69–88.

Nath, R., Cui, X., Nath, D., Graf, H. F., Chen, W., Wang, L., Gong, H., & Li, Q. (2017). CMIP5 multimodal projections of extreme weather events in the humid subtropical Gangetic Plain region of India. *Earth's Future, 5*, 224–239.

Palmer, W.C. (1965) Meteorological drought. Research Paper No 45, U.S. Weather Bureau, Washington, D.C., 58 pp.

Rajeevan, M., & Bhate, J. (2009). A high resolution daily gridded rainfall dataset (1971–2005) for mesoscale meteorological studies. *Current Science, 96*(4), 558–562.

Shah, H. L., & Mishra, V. (2016). Hydrologic Changes in Indian sub-continental river basins (1901-2012). *Journal of Hydrometeorology, 17*, 2667–2687.

Shelton, M. L. (2009). *Hydroclimatology: perspectives and applications*. Cambridge: Cambridge University Press.

Sheng, Y., & Hashino, M. (2007). Probability distribution of annual, seasonal and monthly precipitation in Japan. *Hydrological Sciences Journal, 52*(5), 863–877.

Shibuo, Y., Jarsjö, J., & Destouni, G. (2007). Hydrological responses to climate change and irrigation in the Aral Sea drainage basin. *Geophysical Research Letters, 34*, L21406.

Sinha, D., Syed, T. H., & Reager, J. T. (2019). Utilizing combined deviations of precipitation and GRACE-based terrestrial water storage as a metric for drought characterization: a case study over major Indian river basins. *Journal of Hydrology, 572*, 294–307.

Sposito, G. (2017). Understanding the Budyko equation. *Water., 9*(4), 236.

Srivastava, A. K., Rajeevan, M., & Kshirsagar, S. R. (2009). Development of a high resolution daily gridded temperature data set (1969-2005) for the Indian region. *Atmospheric Scientific Letters, 10*, 249–254. https://doi.org/10.1002/asl.232.

Svoboda, M., LeComte, D., Hayes, M., Heim, R., Gleason, K., Angel, J., & Stephens, S. (2002). The drought monitor. *Bulletin of the American Meteorological Society, 83*(8), 1181–1190.

Thornthwaite, C. W. (1948). An approach toward a rational classification of climate. *Geographical Review, 38*(1), 55–94.

Turc, L. (1954). The water balance of soils, relation between precipitation evaporation and flow. *Ann. Agronomiques., 5*, 491–569.

Vicente-Serrano, S. M., Beguería, S., & López-Moreno, J. I. (2010). A multiscalar drought index sensitive to global warming: the standardized precipitation evapotranspiration index. *Journal of Climate, 23*(7), 1696–1718.

Vicente-Serrano, S. M., López-Moreno, J. I., Lorenzo-Lacruz, J., El Kenawy, A., Azorin-Molina, C., Morán-Tejeda, E., Angulo-Martínez, M., 2011. The NAO impact on droughts in the Mediterranean region. In Hydrological, socioeconomic and ecological impacts of the north Atlantic oscillation in the mediterranean region (pp. 23-40). Springer, Dordrecht.

Vicente-Serrano, S. M., Van-der, S. G., Begueria, S., Azorin-Molina, C., & Lopez Moreno, J. I. (2015). Contribution of precipitation and reference evapotranspiration to drought indices under different climates. *Journal of Hydrology, 526*, 42–54.

Wang, D., & Tang, Y. (2014). A one parameter Budyko model for water balance captures emergent behaviour in Darwinian hydrologic models. *Geophysical Research Letters, 41*, 4569–4577. https://doi.org/10.1002/2014GL060509.

Zhang, L., Hickel, K., Dawes, W. R., Chiew, F. H. S., Western, A. W., & Briggs, P. R. (2004). A rational function approach for estimating mean annual evapotranspiration. *Water Resources Research, 40*, W02502.

Zhang, L., Potter, N., Hickel, K., Zhang, Y. Q., & Shao, Q. X. (2008). Water balance modelling over variable time scales based on the Budyko framework—model development and testing. *Journal of Hydrology, 360*(1-4), 117–131.

Zhang, K., Kimball, J. S., Nemani, R. R., & Running, S. W. (2010). A continuous satellite-derived global record of land surface evapotranspiration from 1983 to 2006. *Water Resources Research, 46*, W09522. https://doi.org/10.1029/2009WR008800.

Zhou, S., Yu, B., Huang, Y., & Wang, G. (2015). The complementary relationship and generation of the Budyko functions. *Geophysical Research Letters, 42*, 1781–1790.